

TASCC-P-94-18

PREPRINT

***TASCC***

See 9439

# ***<sup>50</sup>Fe BETA DECAY***

**V.T. Koslowsky, E. Hagberg, J.C. Hardy, H. Schmeing and I.S. Towner**

*AECL Research, Chalk River Laboratories, Chalk River, Ontario, K0J 1J0, Canada  
FAX: (613) 584-1800*

***Submitted to Phys. Lett. B.***

## **NOTICE**

This report is not a formal publication; if it is cited as a reference, the citation should indicate that the report is unpublished. To request copies our E-Mail address is [TASCC@CRL.AECL.CA](mailto:TASCC@CRL.AECL.CA).

Physical and Environmental Sciences  
Chalk River Laboratories  
Chalk River, ON K0J 1J0 Canada

1994 August



CERN LIBRARIES, GENEVA



## $^{50}\text{Fe}$ BETA DECAY

V.T. Koslowsky, E. Hagberg, J.C. Hardy, H. Schmeing and I.S. Towner

*Chalk River Laboratories, AECL Research,  
Chalk River, Ontario, Canada K0J 1J0  
FAX: (613) 584-1800*

### Abstract

The  $\beta^+$  decay of  $^{50}\text{Fe}$  ( $t_{1/2}=155\pm 11$  ms) has been observed for the first time; it exhibits a superallowed branch ( $77\pm 6\%$ ) to the  $0^+$  ground state of  $^{50}\text{Mn}$  and an allowed branch to the  $650.99\pm 0.06$  keV  $1^+$  state. The energy of the latter state has been precisely determined in order to reduce the uncertainties in previous measurements of the  $Q_{\text{EC}}$ -value difference between the superallowed branches of  $^{50}\text{Mn}$  and  $^{54}\text{Co}$ .



Although the  $T_z=-1$  nucleus  $^{50}\text{Fe}$  was produced via the  $(^4\text{He},^8\text{He})$  reaction in 1977 by Tribble et al.<sup>1)</sup> and its mass determined from the reaction  $Q$  value, its decay properties were not known. This paper describes the first characterization of the  $\beta^+$  decay of  $^{50}\text{Fe}$  and a precise energy measurement of the 651 keV  $1^+$  state in the daughter nucleus,  $^{50}\text{Mn}$ , which is populated by an allowed Gamow-Teller (GT) decay branch from  $^{50}\text{Fe}$ .

The 651 keV state has special significance in linking the  $Q_{\text{EC}}$  values of the superallowed  $0^+ \rightarrow 0^+$ ,  $T=1$   $\beta$ -emitters  $^{50}\text{Mn}$  and  $^{54}\text{Co}$ . A very precise  $Q$ -value difference ( $40.90 \pm 0.16$  keV) has been measured<sup>2)</sup> between the reactions  $^{54}\text{Fe}(^3\text{He},t)^{54}\text{Co}(\text{gs})$  and  $^{50}\text{Cr}(^3\text{He},t)^{50}\text{Mn}^*$  (651 keV) but this could not be converted to an equally precise value for the  $Q_{\text{EC}}$ -value difference between the superallowed branches since the excitation energy of the 651 keV state in  $^{50}\text{Mn}$  was only known to a precision of 0.4 keV<sup>3)</sup>. Precise  $ft$ -value determinations, which include  $Q_{\text{EC}}$ -value measurements, for superallowed  $0^+ \rightarrow 0^+$  transitions impact on important tests of the Standard Model of electroweak interactions<sup>4)</sup>.

We produced the  $^{50}\text{Fe}$  activity by bombarding a stack of three self-supporting natural calcium targets, each 1.6 mg/cm<sup>2</sup> thick and spaced 18 mm apart, with a 51 MeV  $^{12}\text{C}$  beam from the Chalk River TASCC Facility. Because the  $^{50}\text{Fe}$  reaction channel was weakly populated and the expected halflife short, the reaction products recoiling from the targets were quickly transferred to a low-background counting area with a He-jet gas-

transfer system. The target chamber was pressurized to 3 atm, being isolated from the beam line vacuum by a gas-tight 3.2 mg/cm<sup>2</sup>-thick Mo foil through which the beam entered. To reduce activity originating from this foil, it was backed with a 1 mg/cm<sup>2</sup> graphite absorber. Helium, loaded with NaCl aerosol particles, was continuously flushed from the target chamber and transported through a 6.5-m-long, 1-mm-diameter capillary. At the capillary exit, activity-loaded aerosol clusters were collected for 350 ms on a continuous, aluminized-mylar tape which passed through a differentially-pumped collection chamber. Each sample on the tape was then transported, through narrow slits, to a shielded location 16 cm away, where it was counted for 600 ms. The cycle was then repeated. With a gas flow of 20 st.l/min., the estimated time to flush reaction products to the tape was 100 ms; the tape movement to the counting location took a further 60 ms.

At the counting location the sample was positioned between two closely spaced thin plastic  $\beta$  scintillators and viewed in close geometry on one side by a 40% HPGe detector. We greatly reduced interference from Bremsstrahlung and neutron-induced background by accepting only  $\gamma$  rays measured in coincidence with  $\beta$  particles striking the opposite-side scintillator, thus identifying events in which the positron and  $\gamma$  ray travelled in opposite directions;  $\gamma$  rays in coincidence with the near-side scintillator were vetoed. All detectors were shielded from the collection chamber with 46 mm of lead. Energy calibration of the  $\gamma$ -ray spectrum in

the 650 keV region was accomplished with a thin 1.2 kBq  $^{124}\text{Sb}$  source, which was placed between the plastic scintillators within 1 mm of the sample position. Detailed descriptions of the helium-jet system and the counting arrangements appear elsewhere<sup>5)</sup>.

Data were recorded event-by-event for all  $\gamma$  rays detected. Five parameters were recorded per event: the sample number, the time of occurrence within the counting interval, the  $\gamma$ -ray energy and the  $\beta$ - $\gamma$  coincidence time from each of the two  $\beta$  scintillators. The energy dispersion was 0.25 keV/channel and energies up to 2 MeV were recorded. A 10 Hz pulser signal, positioned at about 2 MeV, was used for subsequent dead-time corrections to the observed decay rates.

Two sets of data were acquired: one set with the  $^{124}\text{Sb}$  calibration source present; the other with it absent. The energy spectra recorded in the region of the observed 651 keV  $\gamma$ -ray peak are shown in Figure 1. The  $645.855 \pm 0.002$  keV<sup>6)</sup> peak from  $^{124}\text{Sb}$  and other  $^{124}\text{Sb}$  peaks, not shown, were used to determine the energies of the 651 keV peak and of peaks at 662, 783, 1098, 1283, 1443 and 1945 keV from the decay of  $^{50}\text{Mn}$ , which was produced simultaneously (see Table 1). Subsequently, the  $^{50}\text{Mn}$  peaks were used independently to determine the 651 keV  $\gamma$ -ray energy from the data accumulated with the  $^{124}\text{Sb}$  source absent. Peak centroids were determined by lineshape fitting. These data and additional spectra from the  $^{124}\text{Sb}$  source alone indicate that the background under both the 651 keV peak and

the  $^{124}\text{Sb}$ (646 keV) peak is structureless. However, a weak  $\gamma$ -ray peak at 664 keV from the summing of annihilation radiation with a  $^{49}\text{Cr}$ (153 keV) peak leads to a high-energy tail on the  $^{50}\text{Mn}$ (662 keV) peak. This is accounted for in the energy determinations of the 662 keV and 651 keV  $\gamma$  rays. Our final result for the energy of the latter peak -  $650.99 \pm 0.06$  keV - is given in Table 1. It agrees with, but is much more precise than, the known energy<sup>3)</sup> of the second excited state in  $^{50}\text{Mn}$  ( $E_x=651.1 \pm 0.4$ ). This agreement, together with the short half-life (see next paragraph), establishes  $^{50}\text{Fe}$  as the parent activity.

Figure 2 shows the decay curve of the 651 keV  $\gamma$ -ray peak. Dead-time corrections were determined from the pulser events; the maximum dead-time was about 25%. We analyzed the decay curve first by fitting a one-component exponential decay curve plus constant background to the data. The constant background was found to be consistent with zero and subsequently fixed at that value while the data were re-analyzed for the intensity and decay constant. The half-life we obtained for  $^{50}\text{Fe}$  (see Table 1) was  $155 \pm 11$  ms. As a by-product we also generated a decay curve for  $^{49}\text{Mn}$  by gating on its characteristic  $\gamma$  ray at 272 keV; this yielded a half-life of  $405 \pm 55$  ms in good agreement with an earlier measurement<sup>7)</sup> that yielded  $384 \pm 17$  ms.

From the  $Q_{\text{EC}}$  value and the world average  $\mathcal{F}_t$  value for  $0^+ \rightarrow 0^+ \beta$  transitions<sup>4,9)</sup>, the partial halflife for the superallowed branch to the



ground state of  $^{50}\text{Mn}$  can be reliably determined to be  $202 \pm 8$  ms (see Table 2). By comparison with our measured total half life, this yields a branching ratio of  $77 \pm 6\%$ . Since only one  $\gamma$ -ray peak attributable to  $^{50}\text{Fe}$  decay was observed, it is reasonable to assume that all significant remaining beta strength populates the 651 keV state in  $^{50}\text{Mn}$ ; in that case, the log ft for that transition is determined to be  $3.81 \pm 0.12$ , which establishes it as being allowed. Consequently, the 651 keV state is restricted to  $J^\pi=1^+$  consistent with previous results<sup>3)</sup> which indicated  $J^\pi=1,2^+$ .

Our new value for the excitation energy of the 651 keV state in  $^{50}\text{Mn}$  can now be combined with the earlier reaction Q-value difference measurement<sup>2)</sup> to yield the  $Q_{\text{EC}}$ -value difference between  $^{54}\text{Co}$  and  $^{50}\text{Mn}$ . The result is  $610.09 \pm 0.17$  keV, in which the predominant source of uncertainty now lies with the reaction Q-value difference measurement. This new  $Q_{\text{EC}}$ -value difference is in good agreement with, and supersedes, our former value<sup>2)</sup> which was 3 times less precise. It is also in agreement with the only available  $Q_{\text{EC}}$ -value measurements<sup>10)</sup> for  $^{50}\text{Mn}$  and  $^{54}\text{Co}$  that have accuracies substantially less than  $\pm 1$  keV. They yield a difference of  $609.7 \pm 0.7$  keV. Their consistency is especially valuable in view of a sparseness of the data available for  $^{50}\text{Mn}$  and  $^{54}\text{Co}$  when compared with the six other well-studied  $0^+ \rightarrow 0^+$  superallowed  $\beta$  emitters, which have each had the  $Q_{\text{EC}}$  values determined by several independent groups<sup>4)</sup>.

The Conserved Vector Current (CVC) hypothesis<sup>4)</sup> predicts that the weak vector coupling constant is not renormalized by the nuclear medium; thus, the  $\hat{F}_t$  values of  $^{50}\text{Mn}$  and  $^{54}\text{Co}$  should be identical. A measure of their consistency is given by the R factor, defined in reference 2 to be:

$$R(A,B) = [\hat{F}_t(A) - \hat{F}_t(B)] / \hat{F}_t(B).$$

If the results of this experiment are used to determine  $R(50,54)$ , the result is  $(0.02 \pm 0.14)\%$  which agrees completely with zero as required by CVC.

## References

- 1) R.E. Tribble, J.D. Cossairt, D.P. May and R.A. Kenefick, Phys. Rev. C16 (1977) 917.
- 2) V.T. Koslowsky, J.C. Hardy, E. Hagberg, R.E. Azuma, G.C. Ball, E.T.H. Clifford, W.G. Davies, H. Schmeing, U.J. Schrewe and K.S. Sharma, Nucl. Phys. A472 (1987) 419.
- 3) Nuclear Data Sheets 61 (1990) 1.
- 4) J.C. Hardy, I.S. Towner, V.T. Koslowsky, E. Hagberg and H. Schmeing, Nucl. Phys. A509 (1990) 429.
- 5) E. Hagberg, T.K. Alexander, J. Neeson, V.T. Koslowsky, G.C. Ball, G.R. Dyck, J.S. Forster, J.C. Hardy, J.R. Leslie, H-B. Mak, H. Schmeing and I.S. Towner, Nucl. Phys. A571 (1994) 555.
- 6) Nuclear Data Sheets, 41 (1984) 413.
- 7) J.C. Hardy, H. Schmeing, E. Hagberg, W.L. Perry, J.S. Wills, E.T.H. Clifford, V.T. Koslowsky and I.S. Towner, Phys. Lett. 91B (1980) 207.
- 8) I.S. Towner, private communication.
- 9) I.S. Towner, Nucl. Phys. A540 (1992) 478.
- 10) H. Vonach, R. Glässel, E. Huenges, P. Maier-Komor, H. Rösler and H.J. Scheerer, Nucl. Phys. A278 (1977) 189.

TABLE 1  
SUMMARY OF EXPERIMENTAL DATA

Experimental Conditions	$^{50}\text{Fe}$ Halflife (ms)	$\beta$ -Delayed $\gamma$ -ray energy (keV)	
		$^{50}\text{Fe}$	$^{50}\text{Mn}$
$^{124}\text{Sb}$ present		651.04 $\pm$ 0.06	661.63 $\pm$ 0.02
			783.36 $\pm$ 0.04
			1098.14 $\pm$ 0.10
			1282.68 $\pm$ 0.10
			1443.38 $\pm$ 0.20
1944.7 $\pm$ 0.4			
$^{124}\text{Sb}$ absent		650.93 $\pm$ 0.06	
Average	155 $\pm$ 11	650.99 $\pm$ 0.06 <sup>a)</sup>	

a) Uncertainty inflated by the square root of the normalized  $\chi^2$ .

TABLE 2  
DECAY PROPERTIES OF  $^{50}\text{Fe}$

	Transition to ground state	Transition to 651 keV state
$Q_{\text{EC}}$ value (keV) <sup>1)</sup>	$8152 \pm 61$	$7501 \pm 61$
Statistical rate function, $f$ <sup>8)</sup>	$(1.507 \pm 0.061) \times 10^4$	$(0.953 \pm 0.042) \times 10^4$
Radiative correction, $\delta_{\text{R}}$ (%) <sup>8)</sup>	1.42	1.47
Charge-dependent correction, $\delta_{\text{C}}$ (%) <sup>8)</sup>	0.4	0.4
$\overline{F} = f(1 + \delta_{\text{R}})(1 - \delta_{\text{C}})$	$(1.522 \pm 0.061) \times 10^4$	$(0.963 \pm 0.042) \times 10^4$
World average $\overline{F}t$ value (s) <sup>4, 9)</sup>	$3074.0 \pm 1.0$	
Deduced partial half-life, $t$ (ms)	$202 \pm 8$	
Deduced branching ratio (%)	$77 \pm 6$	$23 \pm 6$
$\log ft$	$3.49 \pm 0.00^{4, 9)}$	$3.81 \pm 0.12$

---

## FIGURE CAPTIONS

Figure 1 Gamma-ray spectra measured in coincidence with positrons from the far-side scintillator and in anti-coincidence with those from the near-side scintillator (see text). The upper spectrum was measured simultaneously with a  $^{124}\text{Sb}$  calibration source. The lower spectrum is without the  $^{124}\text{Sb}$  calibration source.

Figure 2  $^{50}\text{Fe}$  Decay curve for the 651 keV  $\gamma$ -ray peak. A total of 2602 events were counted in 126123 cycles. The average beam current was 600 particle nA, indicating a  $^{50}\text{Fe}$  counting rate of one event per 10 particle  $\mu\text{C}$ .





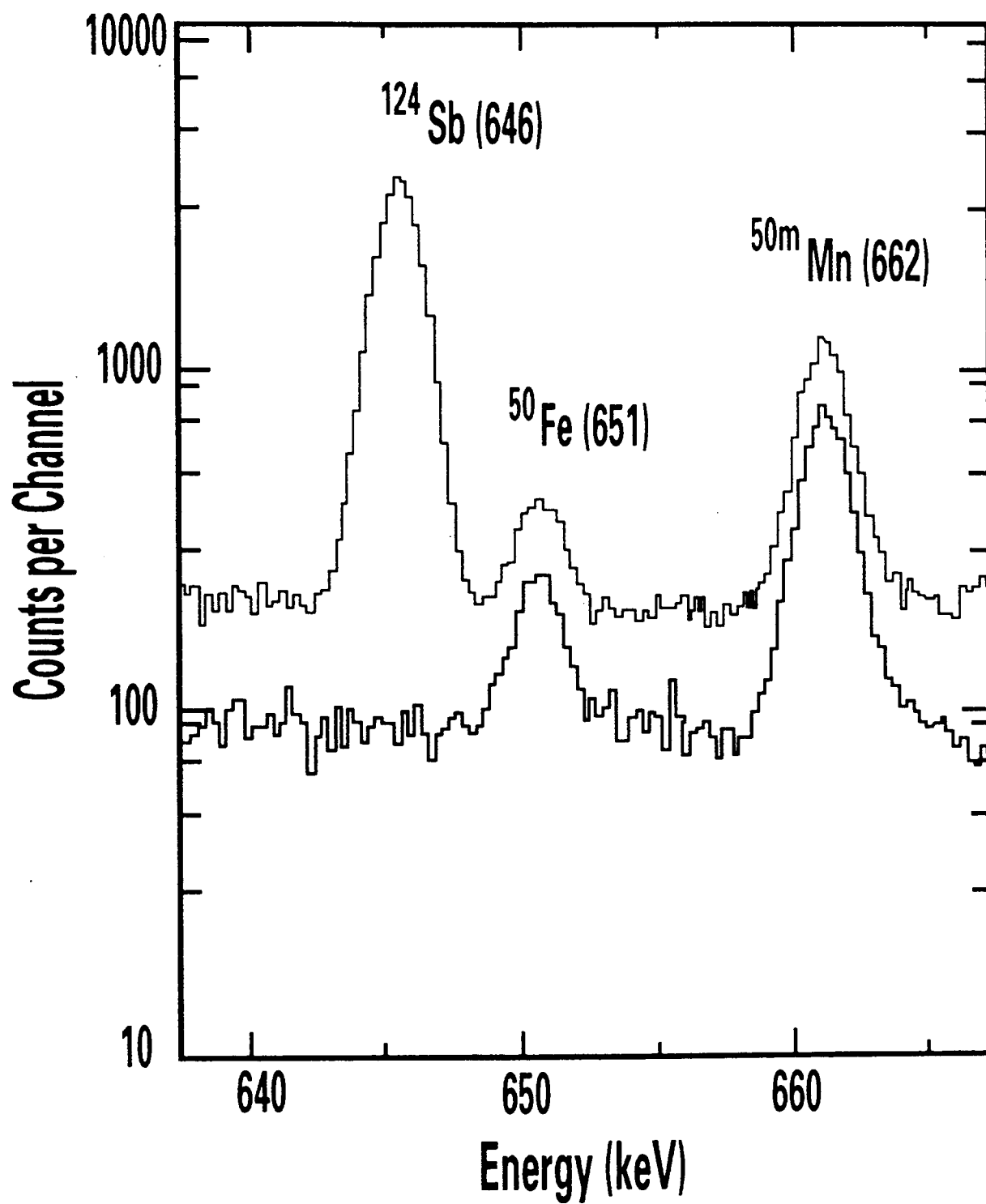


Fig 1

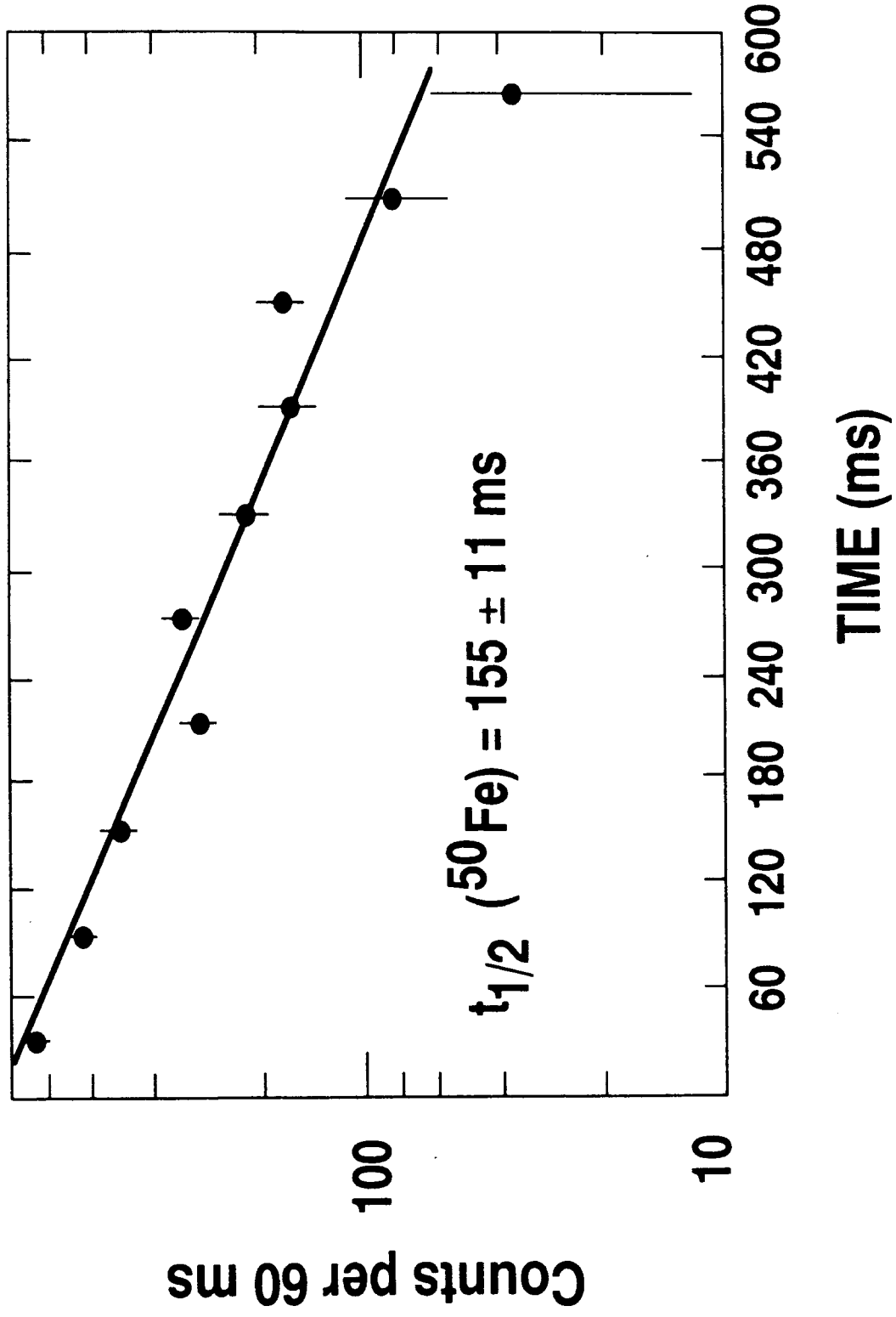


Fig 3





**AECL EACL**

---

**AECL Research**

**EACL Recherche**

---